Thermodynamics of Nucleotide and Non-ATP-Competitive Inhibitor Binding to MEK1 by Circular Dichroism and Isothermal Titration Calorimetry

Catherine K. Smith* and William T. Windsor

Schering-Plough Research Institute, 2015 Galloping Hill Road, Kenilworth, New Jersey 07033

Received September 12, 2006; Revised Manuscript Received November 17, 2006

ABSTRACT: MEK1 is a member of the MAPK signal transduction pathway that responds to growth factors and cytokines. A wealth of information about the enzymatic activity of MEK1, its domain functions, and inhibitor action is available; however, the thermodynamic properties of the interaction between MEK1 and ligands, such as nucleotides and non-ATP-competitive inhibitors, have not been reported. This study describes the thermodynamic parameters for the binding interactions of MEK1, nucleotides, and non-ATP-competitive inhibitor complexes using temperature-dependent circular dichroism (TdCD) and isothermal titration calorimetry (ITC). Non-phosphorylated MEK1 (npMEK1) has a high affinity for both AMP-PNP and ADP ($K_d \sim 2\mu$M). The binding is enthalpically favored and Mg-dependent. The active, phosphorylated form of MEK1 (pMEK1) bound nucleotides with a similar high affinity ($K_d \sim 2\mu$M) and had a thermodynamic profile and Mg-dependence similar to that of the non-phosphorylated form. The non-ATP-competitive MEK1 inhibitors, U0126 and PD0325901, showed no preference for npMEK1 and pMEK1 by TdCD. TdCD results also showed that these inhibitors are more potent in the presence of the nucleotide than in its absence. The ternary complex, MEK1·PD0325901·nucleotide, showed synergistic binding as evidenced by a large, non-additive shift in the midpoint of the protein unfolding transition (T_m). This was apparent for both npMEK1 and pMEK1 using either ADP or AMP-PNP. ITC binding studies confirmed the synergistic binding effect. The ITC-determined affinity of nucleotide (AMP-PNP, ADP) binding to the npMEK1·PD0325901 complex was enhanced nearly 5-fold compared to nucleotide binding to npMEK1 alone. In addition, the affinity of PD0325901 binding to npMEK1·nucleotide complexes was increased nearly 10-fold relative to the affinity of PD0325901 for npMEK1 alone. These are the first thermodynamic binding studies that characterize the affinity of the allosteric non-ATP-competitive inhibitors U0126 and PD0325901 with and without the nucleotide. The results indicate these allosteric inhibitors have a dynamic range in the type of MEK1 activation states and nucleotide complexes that they can bind.

MEK1 is a member of the mitogen activated protein kinase (MAPK) cascade. This highly conserved eukaryotic signaling pathway links cellular responses to extracellular stimuli, such as growth factors and cytokines (*1*, *2*). MAPKs are organized as evolutionarily conserved modules composed of three sequentially activating kinases: an upstream MAPK kinase−kinase (MAPKKK, Raf), which phosphorylates and activates the MAPK kinase (MAPKK, MEK), which in turn phosphorylates and activates the kinase MAPK (ERK) (*2*). The MEK/ERK signaling module is the predominant MAPK pathway mediating responses to both proliferative and differentiating signals (*3*, *4*).

MEK1/2 are dual specificity kinases that activate ERK1/2 via phosphorylation of Thr and Tyr residues in the regulatory activating lip or T-loop (*T*E*Y*) of ERK1/2 (*5*). Unlike many other kinases, MEK1/2 apparently require both the correct phosphorylated T-loop residues and the native ERK1/2 tertiary fold for recognition and activation. MEK1/2 do not phosphorylate ERK1/2 peptides nor do they phosphorylate denatured ERK1/2 (*6*). The interaction between MEK1/2 and ERK1/2 is unusually specific: MEK1/2 are the only known activators of ERK1/2, and ERK1/2 are the only known substrates of MEK1/2 (*1*, *7*).

MEK1/2 are regulated and activated by Raf phosphorylation on two serine residues in the T-loop, Ser218 and Ser222 (*S*M*A*N*S*) (*8*, *9*). Dual phosphorylation on both serine residues is required for activation (*10*). The dephosphorylated forms of MEK1/2 have extremely low activity, which is increased 5000-fold after maximal phosphorylation with c-Raf in a coupled assay (*9*). Substitution of the T-loop serine residues with negatively charged amino acids, such as aspartate or glutamate, partially mimics the phosphorylation modification and results in a constitutively active kinase (*11*−*14*). For example, the specific activity of the S218D/S222D MEK1 is 300-fold greater than the basal activity of the wild-type enzyme (*15*).

As might be expected for a protein kinase that resides within an important growth control pathway, MEK1 is a well-studied pharmacologic target for cancer therapy, and a number of MEK1 inhibitors have been reported (*1*). Many of these inhibitors are non-competitive with ATP and appear to bind in an allosteric site that is distinct from the ATP binding pocket (*1*, *16*). Examples of such MEK1 inhibitors include the non-ATP-competitive inhibitors PD98059, U0126, and PD184352 (*17*−*21*). It has been shown that PD98059

* Corresponding author: Tel: (908) 740-4787. Fax: (908) 740-4844. E-mail: catherine.smith15@spcorp.com.

10.1021/bi061893w CCC: $37.00
Published on Web 01/13/2007

and U0126 compete for the same or overlapping pockets through equilibrium binding experiments using radioactively labeled compounds (*19*). A genetic screen in yeast identified amino acids in MEK1 that affect PD184352 binding and defined a region in the N-terminal domain where this compound likely binds (*20*). The high-resolution crystal structures of MEK1 and MEK2 in a ternary complex with ATP and PD184352-like inhibitors confirmed that the allosteric inhibitor binding site in MEK1 is distinct but adjacent to the ATP binding site (*22*).

An analysis of the MEK1 ternary complex crystal structure indicates that PD184352-like inhibitors "bind and stabilize a naturally occurring inactive conformation of the protein" (*22*). Because the structures of apo, nucleotide only, and phosphorylated MEK1 have not been determined, it is difficult to differentiate between native and inhibitor-induced alterations to the classical kinase fold. Nevertheless, the reported X-ray structure for the non-phosphorylated state in complex with PD184352-like inhibitors (PD313088, PD334581) suggests that these inhibitors can bind to a low activity form of MEK1 with significant conformational changes at the beginning of the activation loop and a shift in the location of helix C (*22*).

Biochemical studies show conflicting data as to whether allosteric MEK1 inhibitors target the active or inactive form of MEK1. In one study, U0126 and PD184352 prevented the activation (hence phosphorylation) of MEK1 rather than blocked its kinase activity (*23*). In a separate study, PD98059 did not inhibit phosphorylated MEK1 but instead appeared to prevent the Raf-mediated activation (i.e., phosphorylation) of wild-type MEK1 (*17*). These two reports suggest that U0126 and PD98059 may preferentially target the inactive form of MEK1. However, in a subsequent report, PD98059 and U0126 preferentially inhibited a recombinant, constitutively activated version of MEK1, ΔN3-S218E/S222D, versus the wild-type (*19*). This result suggests that the inhibitors primarily target the activated form of the kinase. Recently, it was shown that PD184352 did not inhibit MEK phosphorylation by Raf *in vitro* or *in vivo* and was even found to increase MEK1 phosphorylation with increasing inhibitor concentrations (*20*). Thus, the mechanism of inhibition for these non-ATP-competitive inhibitors is still not entirely clear.

A full understanding of MEK1 allosteric inhibition requires knowledge of the structure as well as the thermodynamics of the ligands bound individually and together in a ternary complex. Because the low and high activity kinase forms may adopt different conformations that could impact ligand binding, such studies must be performed with both phosphorylated and non-phosphorylated proteins. In contrast to the structural basis for kinase−inhibitor interactions, our understanding of the thermodynamics of kinase inhibition, particularly allosteric inhibition, is still rudimentary. The thermodynamic properties of MEK1 with different nucleotides and inhibitors have not been previously described. Differences in the affinity of nucleotide binding to the low and high activity states of MEK1 and the effect that non-ATP-competitive inhibitors have on nucleotide binding and specificity have also not been reported.

Here, we describe the thermodynamic characterization of ligand binding for the binary MEK1·nucleotide, binary MEK1·inhibitor and ternary MEK1·inhibitor·nucleotide complexes studied by temperature-dependent circular dichroism (TdCD) and isothermal titration calorimetry (ITC[1]). The non-ATP-competitive inhibitors used in this study are U0126 (*19*) and a PD184352-like analogue, PD0325901, which is currently in Phase II clinical trials (*16*, *24*).

MATERIALS AND METHODS

Materials. PD0325901 was synthesized at Schering-Plough Research Institute. Its identity was confirmed by NMR and LC-MS. U0126 was obtained from Calbiochem (*19*). These two MEK1 inhibitors were selected for study because they represent two different chemotypes, yet they are both allosteric inhibitors that are non-competitive with ATP. Furthermore, the crystal structure of MEK1 in a ternary complex with a PD0325901-like inhibitor and ATP has been reported (*22*). The nucleotides (ATP-γS, AMP-PCP, AMP-PNP, ADP, and AMP) used in this study were obtained from Sigma. Several nucleotides and nucleotide analogues are known to hydrolyze when bound to MEK1 (*25*). LC-MS was used to measure the phosphorylation of ERK2 under the conditions used for these direct binding studies. LC-MS showed that pMEK1 was able to modify ERK2 using ATP or ATP-γS but not AMP-PNP or AMP-PCP as a substrate (data not shown). As a result, our thermodynamic studies used only nucleotides or analogues that did not hydrolyze including AMP-PNP, AMP-PCP, ADP, and AMP. The purity of the nucleotides was found to be >90% pure by LCMS.

MEK1 Protein. The specific details of the expression, purification, and characterization of the MEK1 proteins used in this study have been previously described (*26*). Briefly, human phosphorylated and non-phosphorylated MEK1 were expressed in High-Five insect cells and purified to ∼95% homogeneity using anion exchange and Ni-NTA chromatography followed by gel filtration. Okadaic acid was used during the expression and purification of pMEK1 to prevent dephosphorylation. Lambda phosphatase was used in the purification of npMEK1 to eliminate the adventitious phosphorylation that occurs during expression in insect cells. Western blotting using anti-phospho MEK1 antibodies, activity assays, and LCMS were used to ensure that the pMEK1 preparation was fully active and phosphorylated and contained no unphosphorylated MEK1. Purified pMEK1 was heterogeneously phosphorylated and contained predominantly 2 phosphate moieties with smaller amounts of 1 and 3 phosphates apparent. No unphosphorylated MEK1 was detected in the pMEK1 preparation by LCMS. Similar characterization experiments also showed that no pMEK1 cross-contaminated the npMEK1 preparation. Furthermore, the IC_{50} values for U0126 and PD0325901 for pMEK1 were

[1] Abbreviations: ATP, adenosine 5′- triphosphate; ADP, adenosine 5′-diphosphate; AMP-PNP, adenosine 5′-(β,γ-imido) triphosphate; AMP-PCP, β,γ-methylene adenosine 5′ triphosphate; ATP-γS, adenosine 5′-[γ-thio]-triphosphate; AMP, adenosine monophosphate; CD, circular dichroism; ITC, isothermal titration calorimetry; DMSO, dimethyl sulfoxide; HEPES, *N*-(2-hydroxyethyl) piperazine-*N*′-(2-ethanesulfonic acid); DTT, dithiothreitol; NMR, nuclear magnetic resonance spectroscopy; LC-MS, liquid chromatography mass spectroscopy; DSC, differential scanning calorimetry; Thr, (T) threonine; Ser, (S) serine; Tyr, (Y) tyrosine; Glu, (E) glutamic acid; Asp, (D) aspartic acid; Lys, (K) lysine; Ala, (A) alanine; Met, (M) methionine; Asn, (N) Asparagine.

150nM and ≤43nM, respectively, using both filter-binding and FLASH plate assay formats (Carr, D., personal communication and ref 26 (*26*)). These values are similar to published IC_{50} values of 70 nM (*19*) and 1 nM (*27*), respectively.

Temperature-Dependent Circular Dichroism. The CD experiments were performed on a Jasco J810 spectropolarimeter equipped with a 6-cell piezoelectric temperature controller. Ellipticity was monitored at 230 nm as a function of temperature with a 1 mm path length cell. The scan rate was 1 °C per min with a 4 s response time and 30 s equilibration between measurements. Stock protein was diluted to 5 μM with 25 mM HEPES at pH 7.5, 150 mM NaCl, 10% glycerol, 1 mM $MgCl_2$, 1 mM DTT, and 1% DMSO. The following nucleotides were tested at 0.5 mM concentrations: ATP-γS, AMP-PNP, AMP-PCP, ADP, and AMP. The following compounds were tested at 30 μM concentrations: U0126 (Calbiochem) and PD0325901. Data were analyzed using Jasco software, and the midpoints of the protein unfolding transition (T_m) were reported as the average from three separate experiments.

Calculation of K_d from ΔT_m Determined by TdCD. The thermodynamics of temperature-induced protein unfolding equilibria and how ligand binding impacts protein stability as detected by changes in the midpoint of unfolding (T_m) are well-documented (*28*−*31*). Brandts and Lin provided an elegant description for determining the affinity of ligands from temperature-dependent protein stability studies using differential scanning calorimetry (DSC). Subsequently, the equations used for the DSC study have been applied to TdCD, and the details of how to perform and analyze ligand binding thermal unfolding data from CD to determine binding constants have been previously described (*32*). The following scheme and equations summarize this work and were used to estimate K_d for nucleotide and ligand binding to MEK1 on the basis of the changes these ligands produced in MEK1 T_m. The scheme below describes the ligand-dependent change in the unfolding profile, where L and NL are the free ligand and ligand-bound protein species, respectively, and U is the unfolded protein.

Scheme 1

$$NL \Leftrightarrow N + L \Leftrightarrow U$$

The ligand binding constant (K_L (T_m)) can be calculated at the T_m by the following equation

$$K_L(T_m) = \{\exp\{ -(\Delta H_u(T_0)/R)(1/T_m - 1/T_0) + (\Delta C_{pU}/R)[\ln(T_m/T_0) + (T_0/T_m) - 1]\} - 1\}/[L_{T_m}] \quad (1)$$

where T_0 is the midpoint of unfolding for the unliganded protein, T_m is the midpoint of unfolding in the presence of the ligand, ΔH_u is the enthalpy of protein unfolding, and ΔC_{pU} is the heat capacity associated with protein unfolding. If the value of ΔC_{pU} is small, then changes in T_m are proportional to the logarithm of the binding constant and free-ligand concentration (L_{T_m} at T_m. The equilibrium association constant K_L (T_m) described by eq 1 represents the ligand binding association equilibrium constant that occurs at the elevated T_m value. To estimate the K_L (T) at a lower temperature, such as 20 °C, one must use eq 2.

$$K_L(T) = K_L(T_m)\exp\left\{\left(\frac{-\Delta H_L(T)}{R}\right)\left(\frac{1}{T} - \frac{1}{T_m}\right) + \left(\frac{\Delta C_{pL}}{R}\right)\left[\ln\frac{T}{T_m} + 1 - \frac{T}{T_m}\right]\right\} \quad (2)$$

If estimates for both the enthalpy of binding, ΔH_L, and ligand binding heat capacity, ΔC_{pL}, are available, then the ligand binding constant, K_L (T), can be calculated at any temperature T (assuming that the heat capacity term is temperature independent).

TdCD monitors the loss of folded protein secondary structure (α-helices and β-sheets) as a function of temperature. In non-ideal systems, however, this decreasing CD signal is due to both structural unfolding and irreversible protein aggregation. Large proteins at concentrations necessary for a good signal-to-noise ratio often exhibit this aggregation at higher temperatures, and MEK1 is no exception. As a result, the final observed unfolding profile reflects a combination of both effects. However, it has been suggested that irreversible unfolding may be treated as two discrete steps, where a relatively fast native-to-unfolded reaction ($<10^{-3}$ s^{-1}) is uncoupled from a much slower aggregation step (*29*). Under this condition, an apparently irreversible process may be treated as a reversible unfolding reaction. In application to MEK1 protein unfolding, we assume that the aggregation step is much slower than the native-to-unfolded reaction.

Isothermal Titration Calorimetry. Purified proteins were dialyzed extensively against 50 mM HEPES at pH 7.4, 300 mM NaCl, 1 mM $MgCl_2$, and 1 mM DTT. The protein was diluted to the appropriate concentration (either 10 or 30 μM) with dialysate buffer immediately prior to the experiment. Protein concentrations were measured in 6.7 M guanidine-HCl buffered with 20 mM phosphate at pH 7.0 at 280 nM using an extinction coefficient of 30745 M^{-1} cm^{-1}. Nucleotide solutions of ADP and AMP-PNP were prepared in the dialysis buffer immediately prior to each titration. Nucleotide concentrations were measured using an extinction coefficient of 15400 M^{-1} cm^{-1} at 260 nm for adenosine. Compounds were prepared in 100% DMSO and added such that the final solution contained 1% DMSO. For these titrations, DMSO was added to the protein solution to the same percentage. PD0325901 was used at 100 μM concentration and U0126 was used at 60 μM in all experiments. Both compounds were shown to be soluble at these concentrations under the ITC solution conditions by nephelometry using a Nepheloskan Ascent 100 Nephelometer (Labsystems). For direct nucleotide (AMP-PNP or ADP) binding experiments, 300 μM nucleotide was injected into 30 μM protein; for direct PD0325901 binding experiments, 100 μM compound was injected into 10 μM protein; for nucleotide binding to the MEK1·PD0325901 complex, 300 μM nucleotide + 100 μM PD0325901 were injected into 30 μM protein + 100 μM PD0325901; for PD0325901 binding to the MEK1·nucleotide complex, 100 μM PD0325901 + 0.5 mM nucleotide were injected into 10 μM protein + 0.5 mM nucleotide; and for nucleotide binding to the MEK1·U0126 complex, 300 μM nucleotide + 60 μM U0126 were injected into 30 μM protein + 60 μM U0126. The direct binding of U0126 to protein gave a poor signal, which could not be increased because of compound solubility limitations. For the same reason, the

binding of U0126 to the MEK1·nucleotide complex also gave a poor signal. In the reverse titration (protein in syringe), MEK1 performed aberrantly and seemed to denature at low concentrations while stirring.

ITC experiments were performed with the Microcal MCS-ITC titration calorimeter (North Hampton, MA). Protein and nucleotide solutions were degassed by vacuum aspiration for 5−10 min at room temperature prior to loading the samples in the ITC cell and syringe. All titrations were carried out at 20 °C with a stirring speed of 350 rpm and a 360 s duration between each 18 μL injection. Parallel experiments were performed by injecting the nucleotide into the buffer or the buffer into the protein to determine heats of dilution. The heats of dilution were negligible in all cases and were subtracted from their respective titrations prior to data analysis.

Thermodynamic parameters N (stoichiometry), K_A (association constant), and ΔH (enthalpy change) were obtained by nonlinear least-squares fitting of experimental data using a single-site-binding model of the Origin software package (version 5.0) provided with the instrument. The free energy of binding (ΔG) and entropy change (ΔS) were obtained using the following equations.

$$\Delta G = -RT \ln K_A \quad (3)$$

$$\Delta G = \Delta H - T\Delta S \quad (4)$$

The affinity of the nucleotide to protein and protein/inhibitor complex is given as the dissociation constant ($K_D = 1/K_A$). For each protein−nucleotide−compound interaction, two or three titrations were performed. Titration data were analyzed independently, and the thermodynamic values obtained were averaged.

RESULTS

Nucleotide Binding Studies: Binary Complexes. The ability of npMEK1 and pMEK1 to bind nucleotides was initially examined using temperature-dependent circular dichroism (TdCD). In this method, the loss of protein secondary structure was monitored as a function of temperature. Proteins bound with a ligand become more resistant to thermal unfolding compared to the apo protein because of the additional stabilizing interactions created between the ligand and the protein. It is well documented that the increase in the midpoint of unfolding (T_m) in the presence of a ligand is proportional to the affinity of the ligand (*28*, *31*). These studies have also demonstrated that a dissociation constant (K_d) can be estimated from ligand-induced changes in T_m measured by methods such as differential scanning calorimetry or TdCD (*31*, *32*).

For most kinases, the K_m value for nucleotides ranges between 3 and 100 μM. According to eqs 1 and 2, this K_d range would produce a shift in T_m between 5 and 0.5 °C for the typical kinase (assuming $\Delta H_u = 100{,}000$ cal/mol, [ATP] = 100 μM, and $\Delta H_L = -7{,}000$ cal/mol) (*32*). Nonphosphorylated MEK1 and pMEK1 showed a clear stabilizing shift in T_m relative to apo protein of approximately 3 °C ΔT_m in the presence of 0.5 mM AMP-PNP (Figure 1; Table 1). This result suggested that the nucleotide affinity (K_d at 20 °C) for both the inactive and active states of MEK1 are similar and in the range of ~10 μM (eq 2) (*32*). Other non-hydrolyzable nucleotide analogues, such as AMP-PCP and ATP-γS, produced a similar ΔT_m (data not shown).

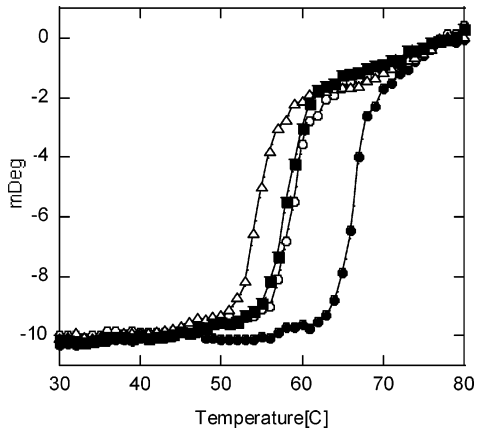

FIGURE 1: CD thermal denaturation curves for npMEK1 ± AMP-PNP ± PD0325901. (△) npMEK1 apo; (○) npMEK1 + AMP-PNP; (■) npMEK1 + PD0325901; (●) ternary complex npMEK1 + AMP-PNP + PD0325901. Ellipticity (mdeg) was measured at 230 nm as a function of temperature (30−80 °C). Protein concentration was 5 μM, AMP-PNP concentration was saturating at 0.5 mM and PD0325901 concentration was 30 μM in 25 mM HEPES at pH 7.4, 150 mM NaCl, 10% glycerol, 1 mM DTT, and 1% DMSO. The temperature was increased 1 °C/min in a 0.1 cm path-length quartz cuvette.

Table 1: Thermodynamic Analysis of Nucleotide and PD0325901 Binding to npMEK1 and pMEK1 by ITC

protein	ligand	ΔT_m[a]	K_d[b] (μM)	ΔG[b] (kcal/mol)	ΔH[b] (kcal/mol)	$T\Delta S$[b] (kcal/mol)
npMEK1	AMP-PNP	3.2	1.6	−7.8	−6.8	1.0
npMEK1	ADP	2.9	2.2	−7.6	−8.7	−1.1
npMEK1	PD0325901	2.8	0.25	−8.9	−7.6	1.3
npMEK1	U0126	2.9				
pMEK1	AMP-PNP	3.1	2.3	−7.6	−7.0	0.6
pMEK1	ADP	3.0	2.1	−7.6	−7.3	0.3
pMEK1	PD0325901	2.8	0.14	−9.2	−7.8	1.4
pMEK1	U0126	3.8				

[a] $\Delta T_m = T_m$ (+ligand) − T_m (apo protein) using 30 μM compound or 0.5 mM nucleotide; T_m pMEK1 = 52.3 °C; T_m npMEK1 = 54.6 °C. [b] Determined at 293 K. K_d values were calculated from ITC-derived K_a. Standard deviation values are from two to three experiments: K_d, 5−10%; ΔH, 3−10%. The stoichiometry of complex formation was 0.9 ± 0.1. The low solubility of U0126 prevented accurate calorimetric determination of U0126 binding thermodynamics to either npMEK1 or pMEK1.

Magnesium plays a critical role in the catalytic cycle of kinases. Although the presence of Mg^{2+} is required for the hydrolysis of ATP by pMEK1, it is unknown whether Mg^{2+} plays a role in the docking of nucleotides in the npMEK1 active site or whether there is a differential role for Mg^{2+} in the low versus high activity forms of MEK1. To address this issue, we examined the effect of Mg^{2+} on the interaction of npMEK1 or pMEK1 with AMP-PNP using TdCD. No nucleotide binding was observed in the absence of Mg^{2+} by TdCD (data not shown). Thus, Mg^{2+} is required for nucleotide binding to both states of MEK1 and was, therefore, included in subsequent experiments.

In many instances, phosphorylated kinases have a higher affinity for ATP than the non-phosphorylated form. Nonphosphorylated MEK1 and pMEK1, however, showed a similar ΔT_m in the presence of AMP-PNP, suggesting that both MEK1 states bind the nucleotide with similar, relatively strong affinities (Table 1). Furthermore, many kinases show

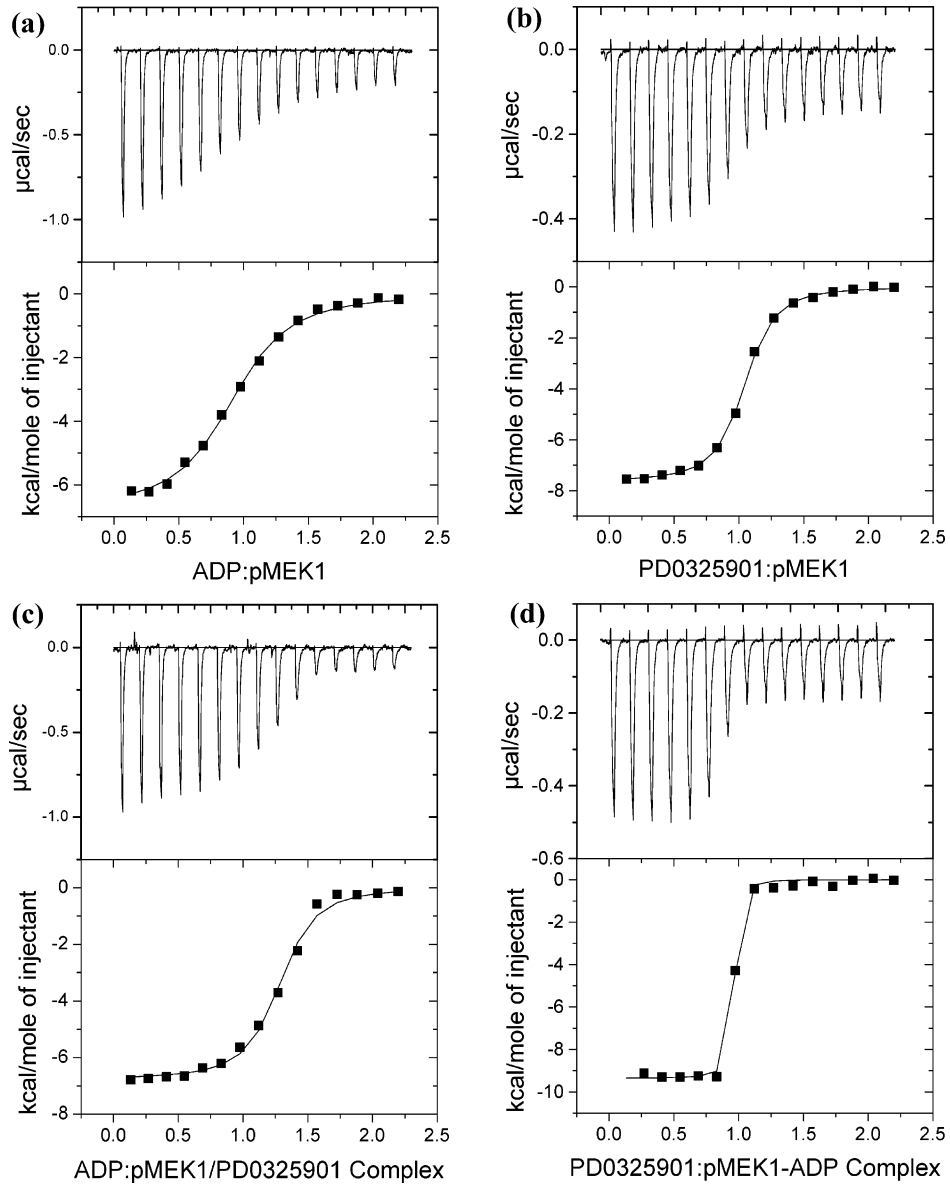

FIGURE 2: Isothermal titration calorimetry: pMEK1 ± ADP ± PD0325901. (Upper panels) Raw isothermal titration calorimetry data demonstrating saturable exothermic evolution of heat upon sequential additions of (a) ADP to pMEK1; (b) PD0325901 to pMEK1; (c) ADP to the pMEK1·PD0325901 complex; and (d) PD0325901 to the pMEK1·ADP complex. (Lower panels) Normalized ITC data for titrations plotted vs the molar ratio of titrant/protein. Data analysis using Origin 5.0 software indicates that the binding data fit well to a single binding-site model.

a lower affinity for the product of the phosphorylation reaction, ADP, than for the triphosphate−nucleotide reactant. The relative affinities for nucleotides generally follow the trend ATP > ADP ≫ AMP. ADP, however, produced ∼2.9 °C ΔT_m for both npMEK1 and pMEK1 compared to the ∼3.2 °C shift with AMP-PNP, suggesting a relatively strong affinity for ADP. No binding was detected for AMP (data not shown).

These nucleotide TdCD binding studies indicate the following: (1) both npMEK1 and pMEK1 bind AMP-PNP with similar, relatively high affinities; (2) neither state of MEK1 shows a difference in specificity for AMP-PMP versus ADP; and (3) both states of MEK1 require Mg^{2+} for nucleotide binding. On the basis of these results, isothermal titration calorimetry (ITC) binding studies were performed to obtain a more complete thermodynamic analysis of nucleotide binding to MEK1 kinase.

Figure 2a shows a representative calorimetric titration of pMEK1 with ADP. The exothermic evolution of heat upon nucleotide injections shown in the upper panel illustrates saturable nucleotide binding by the protein. An analysis of the enthalpy changes versus the ratio of ADP/protein (lower panel) revealed an apparent affinity (K_d) for ADP of 3.0 μM for pMEK1 (Table 1). A similar experiment for npMEK1 gave a K_d of 2.9 μM. Consistent with the TdCD results, both phosphorylated and non-phosphorylated versions of MEK1 bound the nucleotide with similar affinities. The ΔG for binding ADP was approximately −7.6 kcal/mol for both npMEK1 and pMEK1 (Table 1). A comparison of the ΔH and $T\Delta S$ shows that the binding interaction between ADP and both forms of MEK1 is predominantly enthalpic in nature.

Similar ITC results were obtained using AMP-PNP. Consistent with the TdCD results, both npMEK1 and pMEK1

bound AMP-PNP with a relatively strong affinity. The K_d of AMP-PNP for pMEK1 was 2.3 μM and 1.6 μM for npMEK1 (Table 1). The K_d value determined by ITC was further confirmed using a fluorescence polarization assay with mant-ATP, which yielded a similar K_d (3 μM) for npMEK1 (data not shown). A comparison of ΔH and $T\Delta S$ shows that the binding interaction between AMP-PNP and both states of MEK1 is predominantly enthalpic in nature, similar to the interaction with ADP.

To determine if heats of protonation/ionization contribute to the observed ΔH of binding, the ITC experiments with ADP and AMP-PNP were repeated using phosphate buffer instead of HEPES. No significant differences in K_d, entropy, or enthalpy were observed (data not shown), indicating that the apparent ΔH values are similar to the intrinsic ΔH of binding and that the heat of protonation is not significant (*33*, *34*). We further tested the binding of a different ATP analogue, AMP-PCP, using HEPES and phosphate and found no significant differences in the thermodynamics of binding AMP-PCP to npMEK1 or pMEK1 (data not shown).

Non-ATP-Competitive Inhibitor Binding Studies: Binary Complexes. The MEK1 inhibitors, U0126 and PD184352-like compounds such as PD0325901, have been show to be non-competitive with ATP; however, the molecular details of inhibition are not entirely clear. Do these inhibitors bind the MEK1·ADP or MEK1·ATP complexes in a different manner? Do these non-ATP-competitive inhibitors preferentially bind the phosphorylated or non-phosphorylated state of MEK1? To address these aspects of inhibitor function, we measured the direct binding of inhibitors ± nucleotide to npMEK1 or pMEK1 by TdCD and ITC.

In the absence of nucleotides, inhibitors U0126 and PD0325901 bound npMEK1 (using the TdCD method) with a modest ΔT_m of 2.9 and 2.8 °C, respectively (Table 1). Dissociation constant estimates based on these ΔT_m shifts using eq 2 are ~3 μM for both inhibitors (Table 1). The observed ΔT_m for U0126 and PD0325901 binding to pMEK1 are 3.8 and 2.8 °C, respectively, and correspond to K_d values of ~1.5 μM and ~3 μM (Table 1). Thus, it appears that both non-ATP-competitive inhibitors can bind active and inactive MEK1 in the absence of nucleotide.

A more detailed ligand binding analysis was performed by ITC. Figure 2b is an ITC titration of pMEK1 with PD0325901. The binding event is enthalpically favorable and has an ITC K_d of 0.14 μM (Table 1). The ITC titration of npMEK1 with PD0325901 measured a similar affinity (K_d = 0.25 μM, Table 1). The TdCD and ITC methods both suggest that PD0325901 has similar affinities for pMEK1 and npMEK1 and has no significant preference for either activation state. It is not clear why the TdCD-determined K_d for PD0325901 is weaker. The K_d values for PD0325901 determined by ITC and estimated by TdCD in the absence of nucleotide are much higher than the IC_{50} values determined in enzymatic assays which include ATP (IC_{50} PD0325901 ~1nM (*27*); IC_{50} U0126 = 72 nM (*19*)). The poor solubility of U0126 prevented an accurate determination of its affinity to MEK1 by ITC.

Non-ATP-Competitive Inhibitor Binding Studies: Ternary Complexes. Can the binding of nucleotide influence the affinity of U0126 and PD0325901? TdCD binding studies between PD0325901 and MEK1·nucleotide complexes gave a large shift in T_m compared to that given by inhibitor binding to apo MEK1 regardless of the nucleotide used or the phosphorylation state of MEK1 (Figure 1). The ternary complex npMEK1·PD0325901·AMP-PNP had a large ΔT_m of 10.1 °C, and the complex with pMEK1·PD0325901·AMP-PNP gave a similar result (ΔT_m = 11.1 °C). The ΔT_m shifts for the MEK1·PD0325901·ADP complexes were also large for both npMEK1 and pMEK1 (ΔT_m = 9.8, 10.6 °C, respectively) (Table 2). Similar results were observed using AMP-PCP (data not shown). Once again, the affinity of PD0325901 for MEK1 even in the presence of the nucleotide is not influenced by the activation state of the protein. The binding of nucleotides does, however, increase the apparent affinity of PD0325901. This apparent synergistic binding suggested that the inhibitor or nucleotide influences the environment of the other ligand.

The TdCD-based binding of U0126 was also measured for npMEK1·nucleotide or pMEK1·nucleotide complexes. The ΔT_m for U0126 binding to either the npMEK1·AMP-PNP or pMEK1·AMP-PNP complexes was 7.1 and 6.7 °C, respectively. The ΔT_m for U0126 binding to npMEK1·ADP and pMEK1·ADP was 7.0 and 6.3 °C, respectively (Table 4). Similar to the PD0325901 and nucleotide binding studies, the U0126 compound appears to bind with similar affinity to both the unphosphorylated and phosphorylated states of MEK1. In addition, there was no significant difference in affinity for AMP-PNP versus that for ADP. However,

Table 2: Thermodynamic Analysis of Nucleotide Binding to the npMEK1·PD0325901 and pMEK1·PD0325901 Complexes by ITC

preloaded protein complex	ligand	ΔT_m[a]	K_d[b] (μM)	ΔG[b] (kcal/mol)	ΔH[b] (kcal/mol)	$T\Delta S$[b] (kcal/mol)
npMEK1 + PD0325901	AMP-PNP	10.1	0.36	−8.6	−10.2	−1.6
npMEK1 + PD0325901	ADP	9.8	0.34	−8.7	−7.7	1.0
pMEK1 + PD0325901	AMP-PNP	11.1	0.71	−8.3	−10.5	−2.2
pMEK1 + PD0325901	ADP	10.6	0.46	−8.5	−7.5	1.0

[a] $\Delta T_m = T_m$ (+30 μM compound + 0.5 mM nucleotide) − T_m (apo protein); T_m apo pMEK1 = 52.3 °C; T_m apo npMEK1 = 54.6 °C. [b] Determined at 293 K. K_d values were calculated from ITC-derived K_a. Standard deviation values are from two to three experiments: K_d, 5−10%; ΔH, 3−10%. The stoichiometry of complex formation was 1.1 ± 0.1.

Table 3: Thermodynamic Analysis of PD0325901 Binding to the npMEK1·Nucleotide and pMEK1·Nucleotide Complexes

preloaded protein complex	ligand	ΔT_m[a]	K_d[b] (μM)	ΔG[b] (kcal/mol)	ΔH[b] (kcal/mol)	$T\Delta S$[b] (kcal/mol)
npMEK1 + AMP-PNP	PD0325901	10.1	0.018	−10.5	−11.3	−0.8
npMEK1 + ADP	PD0325901	9.8	0.017	−10.4	−7.2	3.2
pMEK1 + AMP-PNP	PD0325901	11.1	≤0.01[c]	−11.3	−10.1	1.2
pMEK1 + ADP	PD0325901	10.6	≤0.01[c]	−11.3	−8.4	2.9

[a] $\Delta T_m = T_m$ (+30 μM compound + 0.5 mM nucleotide) − T_m (apo protein); T_m apo pMEK1 = 52.3 °C; T_m apo npMEK1 = 54.6 °C. [b] Determined at 293 K. [c] The actual fit value (4 nM) is below the sensitivity of the experiment. K_d values were calculated from ITC-derived K_a. Standard deviation values were from two to three experiments: K_d, 5−10%; ΔH, 3−10%. The stoichiometry of complex formation was 1.0 ± 0.1.

Table 4: Thermodynamic Analysis of Nucleotide Binding to npMEK1·U0126 and pMEK1·U0126 Complexes

preloaded protein complex	ligand	ΔT_m[a]	K_d[b] (μM)	ΔG[b] (kcal/mol)	ΔH[b] (kcal/mol)	$T\Delta S$[b] (kcal/mol)
npMEK1 + U0126	AMP-PNP	7.1	2.2	−7.6	−2.0	5.6
npMEK1 + U0126	ADP	7.0	1.3	−7.9	−2.0	5.9
pMEK1 + U0126	AMP-PNP	6.7	2.9	−7.4	−2.9	4.5
pMEK1 + U0126	ADP	6.3	2.5	−7.5	−2.8	4.7

[a] $\Delta T_m = T_m$ (+30 μM ligand + 0.5 mM nucleotide) − T_m (apo protein). [b] Determined at 293 K. K_d values were calculated from ITC-derived K_a. Standard deviation values were from two to three experiments: K_d, 5−10%; ΔH, 3−10%. The stoichiometry of complex formation was 0.9 ± 0.1.

compared to PD0325901, U0126 binding does not appear to be synergistic. Instead, in the presence of the nucleotide, the MEK1·U0126·nucleotide ternary complex produces a ΔT_m that is simply additive with respect to the individual MEK1·U0126 and MEK1·nucleotide binary complexes (Table 1).

Can the synergistic stabilizing effect observed by TdCD with PD0325901 also be detected by ITC for ternary complexes? The synergistic effect should be apparent as an increase in the binding affinity of the nucleotide for MEK1 pre-loaded with PD0325901 relative to binding npMEK1 alone (apo). In other words, we measured the binding of nucleotides to npMEK1 or pMEK1 in the presence of PD0325901 in both the cell and the syringe to ensure that the compound was maintained at a constant concentration throughout the titration (Table 2). Figure 2c shows a representative ITC titration of the pMEK1·PD0325901 complex titrated with a solution of ADP containing an equivalent concentration of PD0325901. The K_d of ADP for the pMEK1·PD0325901 complex was 0.46 μM, which represents a ∼5-fold increase in affinity relative to its K_d for binding apo pMEK1 (2.1 μM) (Tables 1 and 2). Similarly, the affinity of AMP-PNP for pMEK1 in the presence of PD0325901 was increased ∼3-fold (K_d = 0.71 μM) relative to binding apo pMEK1 (K_d = 2.3 μM) (Tables 1 and 2). A similar increase in affinity was detected for both ADP and AMP-PNP (∼6-fold and ∼4-fold, respectively), bound to the npMEK1·PD0325901 complex (Tables 1 and 2). The binding of the nucleotide to the MEK1·PD0325901 complex is primarily enthalpic, where AMP-PNP has a larger ΔH (approximately −10 kcal/mol) than ADP (approximately −7.5 kcal/mol).

To further confirm the synergistic stabilizing effect, the reciprocal ITC experiment was also performed. Here, the binding of PD0325901 to MEK1·nucleotide complexes was measured by ITC (Figure 2d). Synergistic binding should be apparent as an increase in the affinity of the compound to the MEK1·nucleotide complex versus binding to unliganded MEK1 (apo). Additionally, the K_d determined in this experiment for pMEK1 should more closely recapitulate the IC_{50} determined enzymatically because the nucleotide is necessarily present in the kinase assay. The K_d of PD0325901 determined by ITC for pMEK1·AMP-PNP was ≤10nM, which represents a ∼14-fold increase in affinity relative to binding apo pMEK1 (K_d = 140 nM) (Tables 3 and 1). The K_d of the pMEK1·AMP-PNP complex for PD0325901 is close to the enzymatic IC_{50}, ∼1 nM (*27*). Similar results were obtained for the titration of PD0325901 into pMEK1·ADP. The K_d of PD0325901 for npMEK1·AMP-PNP was 18 nM, which represents a ∼14-fold increase in affinity relative to binding apo npMEK1 (K_d = 250 nM, Table 1). Similar results were obtained for the titration of PD0325901 into npMEK1·ADP. The enthalpy of binding PD0325901 to either the npMEK1·AMP-PMP or pMEK1·AMP-PMP complex is approximately −2 to −3 kcal/mol more favorable than the binding of PD0325901 to npMEK1·ADP or pMEK1·ADP. Taken together, the ITC data confirms that PD0325901 and the nucleotide bind synergistically to both pMEK1 and npMEK1. In addition, the high affinity of PD0325901 binding to either the MEK1·AMP-PNP or MEK1·ADP complex recapitulates the potent enzymatic IC_{50} value. Thus, the binding of either nucleotide or inhibitor to MEK1 appears to influence the environment of the binding pocket of the ligand, resulting in an increase in affinity for the ternary complex.

U0126 pre-loaded ITC experiments, similar to those performed with PD0325901 and the nucleotide, were hampered by the low solubility of U0126 and the poor performance of MEK1 in reverse titrations. Nevertheless, ITC experiments yielded data for the titration of the nucleotide into MEK1 complexed with U0126. If the ternary complex were stabilized in an additive manner, the K_d of AMP-PMP or ADP binding to MEK1 should not be significantly affected by the presence of U0126. The K_d values for AMP-PMP binding to npMEK1 and pMEK1 complexed with U0126 were 2.2 and 2.9 μM, respectively (Table 4). The observed K_d values are very similar to the those of AMP-PNP binding to apo npMEK1 or apo pMEK1, which are 1.6 and 2.3 μM, respectively (Table 1). The affinity of ADP was not significantly altered by the presence of U0126 for either npMEK1 or pMEK1. These results support the additive stabilizing effects determined by TdCD for the ternary complex, MEK1·U0126·nucleotide, and are consistent with a previous report that showed that U0126 displays identical affinity for the free enzyme and the MEK·ATP complex (*19*). Of note, the enthalpy of the reaction was significantly lower compared to that of PD0325901, and the predominant effect driving this reaction was entropic (ΔH ∼ −2 to −3 kcal/mol, $T\Delta S$ = 4.5 to 6 kcal/mol).

DISCUSSION

The work described here presents a detailed thermodynamic analysis of nucleotide and non-ATP-competitive inhibitor binding to non-phosphorylated and phosphorylated MEK1. The study yielded both unexpected and interesting results. One of the most dramatic findings was the difference in how U0126 and PD0325901 bound MEK1·nucleotide complexes. PD0325901 showed a synergistic stabilizing effect in the formation of the ternary complex, whereas U0126 showed a straightforward additive stabilization. There are several possible explanations for the origins of the cooperative binding observed. One possibility, guided by the MEK1 crystal structure (*22*), is that PD0325901 mediates additional direct interactions between the protein, nucleotide, and magnesium. As a non-cooperative binder, however, U0126 probably makes no or little contact with the nucleotide and binds MEK1 as an independent moiety. A second

possibility is that MEK1 is a dynamic structure that can adopt multiple conformations that exhibit different nucleotide binding affinities. In this case, PD0325901 would induce a tight nucleotide binding conformation in MEK1, whereas U0126 would not. Of course, these two explanations are not mutually exclusive: PD0325901 may induce a conformational change in MEK1 that both promotes tighter nucleotide binding and allows for additional direct stabilizing interactions as well.

The pre-loaded ITC experiments support the idea that the synergistic binding stems from the creation of additional direct interactions between PD0325901 and AMP-PNP. In this regard, it is instructive to calculate the enthalpic and entropic sources of the relative change in free energy ($\Delta\Delta G$) associated with the binding of a ligand to the binary complex versus that to MEK1 alone.[2] A favorable increase in enthalpy is the major source of increased favorable $\Delta\Delta G$ in the binding of AMP-PNP to MEK1·PD0325901 versus AMP-PNP binding to apo MEK1. Specifically, the $\Delta\Delta H$ for AMP-PNP binding to npMEK1·PD0325901 versus that to apo MEK1 is −3.4 kcal/mol. For AMP-PNP binding pMEK1·PD0325901, the $\Delta\Delta H$ is −3.5 kcal/mol. This observed increase in enthalpic interactions for AMP-PNP binding suggests that additional favorable bonds are created between the protein, nucleotide, and compound. The entropic contributions to this binding event are unfavorable with a $\Delta\Delta S$ of −2.6 and −2.8 kcal/mol for npMEK1·PD0325901 and pMEK1·PD0325901, respectively. A similar thermodynamic pattern was observed in the pre-loaded ITC titrations of PD0325901 into MEK1·AMP-PNP complexes.

The crystal structure of the ternary complex of MEK1·ATP·PD0318088, a PD0325901-like compound, supports the thermodynamic results. In this structure, a network of stabilizing interactions was formed between MEK1, ATP, Mg^{2+}, and PD0318088 (*22*). The compound clearly mediates interactions between the protein and tri-nucleotide, consistent with the synergistic stabilization observed and the predominant enthalpic contribution to $\Delta\Delta G$ measured.

In contrast to AMP-PNP, ADP binds MEK1·PD0325901 complexes with a $\Delta\Delta G$ dominated by favorable entropic contributions. Specifically, the $\Delta\Delta S$ values for ADP binding to npMEK1·PD0325901 and pMEK1·PD0325901 (relative to ADP binding apo MEK1) are 2.1 and 0.7 kcal/mol, respectively. Little or no favorable change in enthalpy is observed with ADP binding to MEK1 complexes: The $\Delta\Delta H$ values for ADP binding to npMEK1·PD0325901 and pMEK1·PD0325901 are 1.0 and −0.2 kcal/mol, respectively. Pre-loaded ITC titrations of PD0325901 into MEK1·ADP also show a similar thermodynamic pattern ($\Delta\Delta S = 1.9$ and 1.5 kcal/mol, and $\Delta\Delta H = 0.4$ and −0.6 kcal/mol for npMEK1 and pMEK1, respectively).

The different balance of entropic and enthalpic factors that contribute to ADP and AMP-PNP binding to MEK1·PD0325901 complexes suggests that there may be structural differences for each ternary complex. Whether the changes in entropy upon AMP-PNP or ADP binding reflect a global conformational change in MEK1 or a change in the ordering of water, individual side-chains, or any of the small molecules involved cannot be gleaned from the thermodynamic analysis alone. To date, there are no crystal structures available for apo MEK1 or for binary MEK1·nucleotide complexes. Without these additional structures for comparison, it is difficult to definitively address whether PD0325901-like compounds also induce different conformational changes in MEK1 in response to ADP or AMP-PNP binding.

Nevertheless, a closer analysis of the available MEK1 structure can suggest some interesting possibilities. In this structure, the beta phosphate of ATP simultaneously interacts with the hydroxyl groups of PD0318088, the catalytic lysine of MEK1 (K98), Asp 207, and Mg^{2+}. It was, therefore, not surprising that PD0325901 did not discriminate between MEK1·AMP-PNP and MEK1·ADP complexes in the binding studies presented here and exhibited a similar affinity for each nucleotide complex. The ΔH for PD0325901 binding to MEK1·AMP-PNP was much higher (−10 to −11 kcal/mol) than that to the MEK1·ADP complex (−7 to −8 kcal/mol), which implies that there are distinct hydrogen bonds and van der Waal interaction differences. The opposite entropic contributions of ADP and AMP-PNP binding to MEK1·PD0325901 complexes suggest that MEK1 arrives at these different ternary complexes in structurally distinct ways. It will be interesting to learn how the MEK1 ternary complex structure accommodates and utilizes the beta and alpha phosphates of ADP in the synergistic binding of PD0325901-like inhibitors.

Although no crystal structure is available for MEK1·nucleotide·U0126 complexes, it seems unlikely that there are any interactions between U0126 and the nucleotide. MEK1 bound U0126 and nucleotide in an additive stabilizing mode, where the ΔT_m of the complex equaled the sum of the ΔT_m values of each binary complex. No significant difference in nucleotide binding affinity for the MEK1·U0126 complex versus that for apo MEK1 was detected by ITC. The balance of entropic and enthalpic contributions to U0126 binding was similar for both nucleotides and both activation forms of the protein. The lack of discrimination between ADP and AMP-PNP is consistent with the manner of additive binding. Any conformational changes that MEK1 may undergo in response to binding AMP-PNP versus ADP did not appear to influence the affinity of this inhibitor bound in the allosteric site.

Another interesting finding was that the activation state of MEK1 did not significantly modulate the binding of binary or ternary complexes. Non-phosphorylated and phosphorylated MEK1 bound AMP-PNP and ADP with similar and relatively high affinities ($K_d \sim 2\ \mu M$). In the pre-loaded ITC experiments, the binding of either AMP-PNP or ADP to the binary complexes (npMEK1·PD0325901 and pMEK1·PD0325901 or npMEK1·U0126 and pMEK1·U0126) resulted in very similar affinities. It is more difficult to evaluate the effect of active or inactive states on the affinity for PD0325901 binding to MEK·nucleotide complexes in the ITC studies because the affinity was very high for pMEK1·nucleotide ($K_d \leq 10$ nM) and beyond the sensitivity of these experiments (Table 3). However, the TdCD method showed that the ΔT_m values for the ternary complexes, npMEK1·nucleotide·PD0325901 and pMEK1·nucleotide·PD0325901, were slightly different (∼10 and ∼11 °C, respectively). It appears that in the context of a ternary complex, PD0325901

[2] $\Delta\Delta G = \Delta G_{binary} - \Delta G_{apo}$; $\Delta\Delta H = \Delta H_{binary} - \Delta H_{apo}$; $\Delta\Delta S = \Delta S_{binary} - \Delta S_{apo}$, where ΔG_{binary}, ΔH_{binary} and ΔS_{binary} refer to the binding of ligand to a pre-loaded binary MEK1 complex and ΔG_{apo}, ΔH_{apo} and ΔS_{apo} refer to the binding of that same ligand directly to apo MEK1.

showed a slightly higher affinity for pMEK1·nucleotide complexes. Nevertheless, the affinity for npMEK1·nucleotide complexes was quite high (K_d = 18 nM), and the effect of the active/non-active state status of MEK1 on the affinity of ligand binding is not all or nothing. Although U0126 showed a preference for binding pMEK1 in the absence of nucleotides by TdCD, this differential was abrogated when nucleotides were included. In both TdCD and ITC experiments, U0126 bound with nearly the same affinity to pMEK1·nucleotide and npMEK1·nucleotide complexes. One of the consequences of the ability of these non-ATP-competitive inhibitors to bind the inactive state is that they have the mechanistic potential to prevent MEK1 phosphorylation by the upstream activating kinase Raf. Conversely, because the inhibitors also bound the phosphorylated state of MEK1, they could functionally prevent the phosphorylation of its substrate, ERK2.

There are many non-ATP-competitive inhibitors that bind MEK1, including U0126, PD0325901, PD184352, PD98059, ARRY-142886, MEK inhibitor 1, and MEK inhibitor 2 (*1*, *17*−*21*, *35*−*37*). The nature of the allosteric pocket that binds these inhibitors has been described in the literature by mutational and crystallographic studies (*20*, *22*). Apparently, the site accommodates a variety of chemotypes and molecular sizes. However, does this allosteric pocket in MEK1 serve a natural function in the cell? How many other kinases contain a similar pocket? Can appropriate inhibitors promote and access this pocket in other kinases? Perhaps this site could be leveraged to obtain or enhance specificity for kinase inhibitors.

ACKNOWLEDGMENT

We thank Thomas Hesson for performing the fluorescence polarization assays, Jesse K. Wong for synthesizing PD0325901, Dr. Vincent Madison and Tim Fedak for assistance with the graphical representation of this work, and Dr. Hung V. Le and Dr. Paul Kirschmeier for critical reading of the manuscript.

REFERENCES

1. English, J., and Cobb, M. (2002) Pharmacological inhibitors of MAPK pathways, *Trends Pharmacol. Sci. 23*, 40−45.
2. Pearson, G., Robinson, F., Beers-Gibson, T., Xu, B., Karandikar, M., Berman, K., and Cobb, M. H. (2001) Mitogen-activated protein (MAP) kinase pathways: regulation and physiological functions, *Endocr. Rev. 22*, 153−183.
3. Sears, R. C., and Nevins, J. R. (2002) Signaling networks that link cell proliferation and cell fate, *J. Biol. Chem. 277*, 11617−11620.
4. Lewis, T. S., Shapiro, P. S., and Ahn, N. G. (1998) Signal transduction through MAP kinase cascades, *Adv. Cancer Res. 74*, 49−139.
5. Payne, D. M., Rossomando, A. J., Martino, P., Erickson, A. K., Her, J. H., Shabanowitz, J., Hunt, D. F., Weber, M. J., and Sturgill, T. W. (1991) Identification of the regulatory phosphorylation sites in pp42/mitogen-activated protein kinase (MAP kinase), *EMBO J. 10*, 885−892.
6. Seger, R., Ahn, N. G., Posada, J., Munar, E. S., Jensen, A. M., Cooper, J. A., Cobb, M. H., and Krebs, E. G. (1992) Purification and characterization of mitogen-activated protein kinase activator(s) from epidermal growth factor-stimulated A431 cells, *J. Biol. Chem. 267*, 14373−14381.
7. Robbins, D. J., Zhen, E., Owaki, H., Vanderbilt, C. A., Ebert, D., Geppert, T. D., and Cobb, M. H. (1993) Regulation and properties of extracellular signal-regulated protein kinases 1 and 2 in vitro, *J. Biol. Chem. 268*, 5097−5106.
8. Resing, K. A., and Ahn, N. G. (1998) Deuterium exchange mass spectrometry as a probe of protein kinase activation. Analysis of wild-type and constitutively active mutants of MAP kinase kinase-1, *Biochemistry 37*, 463−475.
9. Alessi, D. R., Saito, Y., Campbell, D. G., Cohen, P., Sithanandam, G., Rapp, U., Ashworth, A., Marshall, C. J., and Cowley, S. (1994) Identification of the sites in MAP kinase kinase-1 phosphorylated by p74raf-1, *EMBO J. 13*, 1610−1619.
10. Zheng, C.-F., and Guan, K.-L. (1994) Activation of MEK family kinases requires phosphorylation of two conserved Ser/Thr residues, *EMBO J. 13*, 1123−1131.
11. Brunet, A., Pages, G., and Pouyssegur, J. (1994) Constitutively active mutants of MAP kinase kinase (MEK1) induce growth factor-relaxation and oncogenicity when expressed in fibroblasts, *Oncogene 9*, 3379−3387.
12. Cowley, S., Paterson, H., Kemp, P., and Marshall, C. J. (1994) Activation of MAP kinase kinase is necessary and sufficient for PC12 differentiation and for transformation of NIH 3T3 cells, *Cell 77*, 841−852.
13. Mansour, S. J., Matten, W. T., Hermann, A. S., Candia, J. M., Rong, S., Fukasawa, K., Vande Woude, G. F., and Ahn, N. G. (1994) Transformation of mammalian cells by constitutively active MAP kinase kinase, *Science 265*, 966−970.
14. Huang, W., Kessler, D. S., and Erikson, R. L. (1995) Biochemical and biological analysis of Mek1 phosphorylation site mutants, *Mol. Biol. Cell 6*, 237−245.
15. Mansour, S. J., Candia, J. M., Matsuura, J. E., Manning, M. C., and Ahn, N. G. (1996) Interdependent domains controlling the enzymatic activity of mitogen-activated protein kinase kinase 1, *Biochemistry 3*, 15529−15536.
16. Herrera, R., and Sebolt-Leopold, J. S. (2002) Unraveling the complexities of the Raf/MAP kinase pathway for pharmacological intervention, *Trends Mol. Med. 8*, S27−S31.
17. Alessi, D. R., Cuenda, A., Cohen, P., Dudley, D. T., and Saltiel, A. R. (1995) PD 098059 is a specific inhibitor of the activation of mitogen-activated protein kinase kinase in vitro and in vivo, *J. Biol. Chem. 270*, 27489−27494.
18. Dudley, D. T., Pang, L., Decker, S. J., Bridges, A. J., and Saltiel, A. R. (1995) A synthetic inhibitor of the mitogen-activated protein kinase cascade, *Proc. Natl. Acad. Sci. U.S.A. 92*, 7686−7689.
19. Favata, M. F., Horiuchi, K. Y., Manos, E. J., Daulerio, A. J., Stradley, D. A., Feeser, W. S., Van-Dyk, D. E., Pitts, W. J., Earl, R. A., Hobbs, F., Copeland, R. A., Magolda, R. L., Scherle, P. A., and Trzaskos, J. M. (1998) Identification of a novel inhibitor of mitogen-activated protein kinase kinase, *J. Biol. Chem. 273*, 18623−18632.
20. Delaney, A. M., Printen, J. A., Huifen, C., Fauman, E. B., and Dudley, D. T. (2002) Identification of a novel mitogen-activated protein kinase kinase activation domain recognized by the inhibitor PD184352, *Mol. Cell. Biol. 22*, 7593−7602.
21. Sebolt-Leopold, J. S., Dudley, D. T., Herrera, R., Van Becelaere, K., Wiland, A., Gowan, R. C., Tecle, H., Barrett, S. D., Bridges, A., Przybranowski, S., Leopold, W. R., and Saltiel, A. R. (1999) Blockade of the MAP kinase pathway suppresses growth of colon tumors in vivo, *Nat. Med. 5*, 810−816.
22. Ohren, J. F., Chen, H., Pavlovsky, A., Whitehead, C., Zhang, E., Kuffa, P., Yan, C., McConnell, P., Spessard, C., Banotai, C., Mueller, W. T., Delaney, A., Omer, C., Sebolt-Leopold, J., Dudley, D. T., Leung, I. K., Flamme, C., Warmus, J., Kaufman, M., Barrett, S., Tecle, H., and Hasemann, C. A. (2004) Structures of human MAP kinase kinase 1 (MEK1) and MEK2 describe novel noncompetitive kinase inhibition, *Nature Struct. Mol. Biol. 11*, 1192−1197.
23. Davies, S. P., Reddy, H., Caivano, M., and Cohen, P. (2000) Specificity and mechanism of action of some commonly used protein kinase inhibitors, *Biochem. J. 351*, 95−105.
24. Solit, D. B., Garraway, L. A., Pratilas, C. A., Sawai, A., Getz, G., Basso, A., Ye, Q., Lobo, J. M., She, Y., Osman, I., Golub, T. R., Sebolt-Leopold, J., Sellers, W. R., and Rosen, N. (2006) BRAF mutation predicts sensitivity to MEK inhibition, *Nature 439*, 358−362.
25. Khokhlatchev, A. V., Canagarajah, B., Wilsbacher, J., Robinson, M., Atkinson, M., Goldsmith, E., and Cobb, M. H. (1998) Phosphorylation of the MAP kinase ERK2 promotes its homodimerization and nuclear translocation, *Cell 93*, 605−615.
26. Smith, C. K., Carr, D., Mayhood, T. W., Jin, W., Gray, K., and Windsor, W. T. (2006) Expression and purification of phosphorylated and non-phosphorylated human MEK1, *Protein Expr. Purif.*, in press.

27. Sebolt-Leopold, J. S., and Herrera, R. (2004) Targeting the mitogen-activated protein kinase cascade to treat cancer, *Nat. Rev. Cancer 12*, 937−947.
28. Waldron, T. T., and Murphy, K. P. (2003) Stabilization of proteins by ligand binding: application to drug screening and determination of unfolding energetics, *Biochemistry 42*, 5058−5064.
29. Pantoliano, M. W., Petrella, E. C., Kwasnoski, J. D., Lobanov, V. S., Myslik, J., Graf, E., Carver, T., Asel, E., Springer, B. A., Lane, P., and Salemme, F. R. (2001) High-density miniaturization thermal shift assays as a general strategy for drug discovery, *J. Biomol. Screening 6*, 429−440.
30. Matulis, D., Kranz, J. K., Salemme, F. R., and Todd, M. J. (2005) Thermodynamic stability of carbonic anhydrase: measurements of binding affinity and stoichiometry using ThermoFluor, *Biochemistry 44*, 5258−5266.
31. Brandts, J. F., and Lin, L. N. (1990) Study of strong to ultratight protein interactions using differential scanning calorimetry, *Biochemistry 29*, 6927−6940.
32. Mayhood, T. W., and Windsor, W. T. (2005) Ligand binding affinity determined by temperature-dependent circular dichroism: cyclin-dependent kinase 2 inhibitors, *Anal. Biochem. 345*, 187−197.
33. Murphy, K. P., Xie, D., Garcia, K. C., Amzel, L. M., and Friere, E. (1993) Structural energetics of peptide recognition: angiotensin II/antibody binding, *Proteins 15*, 113−120.
34. Gomez, J., and Friere, E. (1995) Thermodynamic mapping of the inhibitor site of the aspartic protease endothiapepsin, *J. Mol. Biol. 252*, 337−350.
35. Kohno, M., and Pouyssegur, J. (2006) Targeting the ERK signaling pathway in cancer therapy, *Anal. Med. 38*, 200−211.
36. Bakare, O., Ashendel, C. L., Peng, H., Zalkow, L. H., and Burgess, E. M. (2003) Synthesis and MEK1 inhibitory activities of imido-substituted 2-chloro-1,4-naphthoquinones, *Bioorg. Med. Chem. 11*, 3165−3170.
37. Wityak, J., Hobbs, F. W., Gardner, D. S., Santella, J. B. r., Petraitis, J. J., Sun, J. H., Favata, M. F., Daulerio, A. J., Horiuchi, K. Y., Copeland, R. A., Scherle, P. A., Jaffe, B. D., Trzaskos, J. M., Magolda, R. L., Trainor, G. L., and Duncia, J. V. (2004) Beyond U0126. Dianion chemistry leading to the rapid synthesis of a series of potent MEK inhibitors, *Bioorg. Med. Chem. Lett. 14*, 1483−1486.

BI061893W